NOTE
Pathology

Choroid plexus carcinoma with neuronal and glial differentiation in a 7-week-old male Sprague-Dawley rat

Mari INOHANA[1], Ayumi EGUCHI[1], Misato NAKAMURA[1], Rei NAGAHARA[1], Yosuke WATANABE[1,2], Toshinori YOSHIDA[1]* and Makoto SHIBUTANI[1]

[1]Laboratory of Veterinary Pathology, Tokyo University of Agriculture and Technology, 3-5-8 Saiwai-cho, Fuchu-shi, Tokyo 183-8509, Japan
[2]Pathogenetic Veterinary Science, United Graduate School of Veterinary Sciences, Gifu University, 1-1 Yanagido, Gifu-shi, Gifu 501-1193, Japan

ABSTRACT. We describe a case of choroid plexus carcinoma arising in the cerebrum of a 7-week-old male Sprague-Dawley rat. The tumor mass occupied the right lateral ventricle of the cerebrum. Histological analyses revealed that the epithelial tumor cells had proliferated in tubular, cribriform, papillary and solid growth patterns in the vicinity of the choroid plexus, with slight invasion into the cerebrum parenchyma. We divided the tumor cells into cuboidal, elongated and intermediate cells. Immunohistochemical studies showed that these tumor cells expressed relatively high levels of cytokeratin AE1/AE3, vimentin and glial fibrillary acidic proteins, and low levels of nestin, oligodendrocyte transcription factor and doublecortin proteins. The present case was diagnosed as a choroid plexus carcinoma with neuronal and glial differentiation.

KEY WORDS: choroid plexus, nestin, OLIG2, rat

Choroid plexus tumors are characterized by the proliferation of epithelial cells arising from the choroid plexus and divided into two types, papillomas and carcinomas [10]. These tumors are composed of well to poorly developed papillary formations in an arboriform pattern. Choroid plexus tumors have been infrequently reported in dogs and rats where the incidence of choroid plexus tumors is found to be 0.1% and less than 0.1%, respectively [11, 16]. In rats, only three choroid plexus papillomas [4, 15, 18] and three choroid plexus carcinoma cases [13–15] have been reported to date. In a 14-week-old female Donryu rat and a 2-year-old female Sprague-Dawley (SD) rat, choroid plexus carcinoma cells expressed cytokeratin [13, 14], but not vimentin, glial fibrillary acidic protein (GFAP) and S-100 [14]. Herein, we report a 7-week-old male SD rat with a choroid plexus tumor in the cerebrum with the expression of mesenchymal, neuronal and glial cell markers.

The affected animal was a specific pathogen-free male SD rat purchased at 4-week of age (Japan SLC, Inc., Shizuoka, Japan) that was housed in a barrier-sustained animal room with controlled temperature (22 ± 3°C), humidity (50 ± 20%) and illumination (12 hr light/dark cycle). The rat had been allocated to the experimental group of a 14-day study of N-nitroso-N-methylurea (MNU) treatment (15 mg/kg/day, p.o.). No clinical abnormalities and body weight change were observed during the study. All the procedures in this study were conducted in compliance with the Guidelines for Proper Conduct of Animal Experiments (Science Council of Japan, June 1, 2006), and the protocols were approved by the Animal Care and Use Committee of the Tokyo University of Agriculture and Technology. The rat was deeply anesthetized with CO_2/O_2 and then killed by exsanguination at the end of the study. The brain was removed and weighed. The absolute weight of the brain was 1.98 g, slightly heavier than the brain of the other animals (1.80–1.92 g, N=3). The brain was fixed in methacarn (methanol:acetic acid:chloroform=6:1:3), and the tumor mass was observed in the cut surface of the cerebrum after fixation. A well-circumscribed, white to pale red, lobular mass, approximately 5 mm in diameter, was located in the right lateral ventricle of the cerebrum; the mass was expanding into the surrounding tissues (Fig. 1). After embedding the brain in paraffin, 3-μm sections were prepared and stained with hematoxylin and eosin (HE) and Masson trichrome (MT). For immunohistochemical studies, we used the avidin-biotin-peroxidase complex method with the primary antibodies listed in Table 1. The chromogen employed was 3,3′-diaminobenzidine, and hematoxylin was used as a nuclear counterstain. As positive control tissues, neurons, glial cells, choroid plexus epithelial cells and ependymal lining were used in the same sections. For negative controls, the primary antibody was replaced with non-immunized sera.
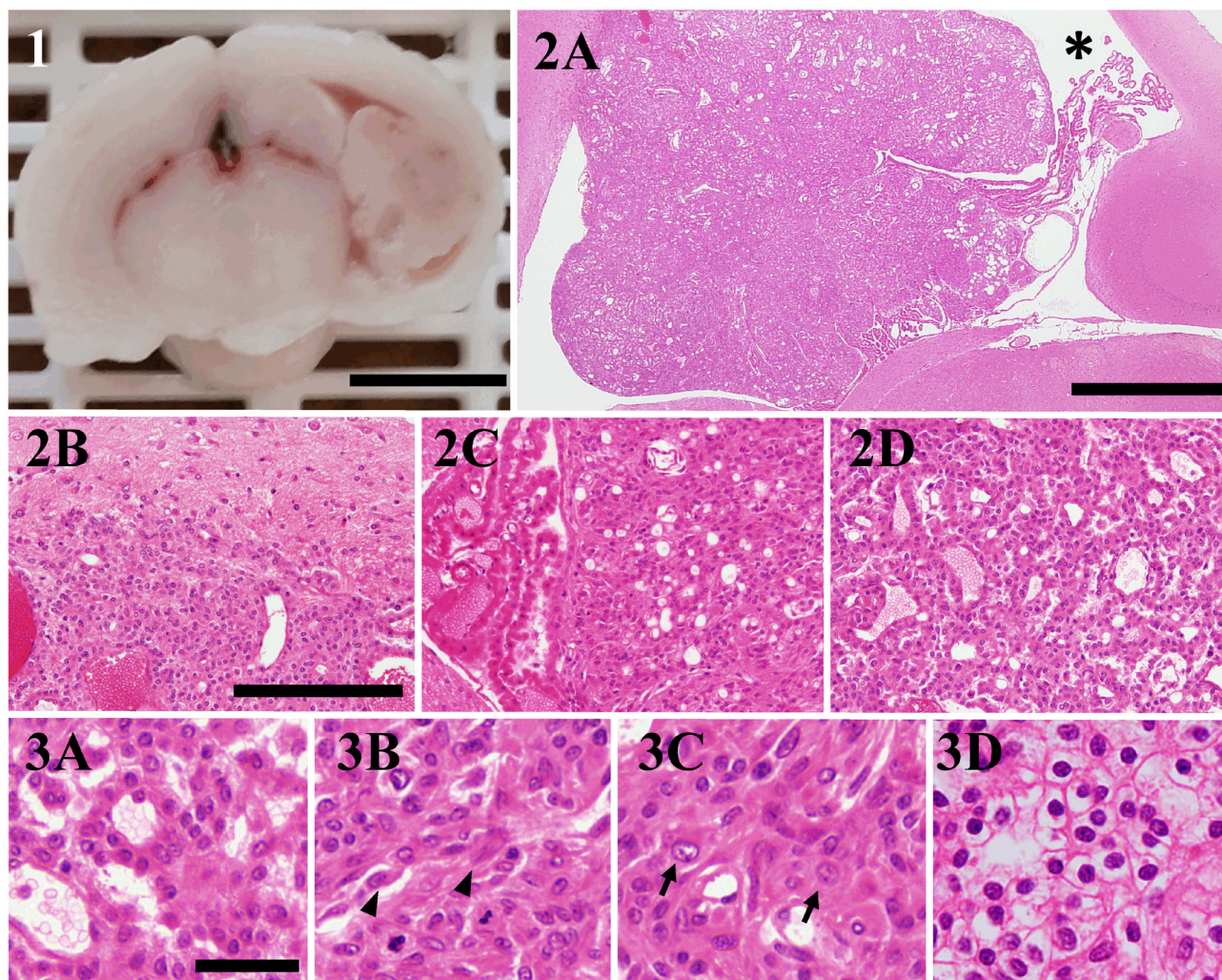
The histopathological examination showed that the tumor mass was located in the right lateral ventricle of the cerebrum (Fig. 2A) and a part of the tumor mass was directly connected to the choroid plexus (Fig. 2A, asterisk). Another part of the tumor mass

Fig. 1. Macroscopic appearance of the tumor mass located in the right lateral ventricle of the cerebrum in the cut surface of the brain. The scale shows a length of 5 mm.

Fig. 2. Histological appearance of the tumor on hematoxylin and eosin staining. At low magnification, the tumor is shown positioned in the right lateral ventricle of the cerebrum (A) and a part of the tumor mass is shown to be directly connected to the choroid plexus (A, asterisk). Bar=1 mm. At medium magnification, a part of tumor is partially attached to the brain parenchyma (B). The tumor cells show solid (B), papillary (C, left side), cribriform (C, right side) and tubular (D) growth patterns. Bar=200 μm.

Fig. 3. Histological appearance of the tumor at high magnification. Tumor cells were stained with hematoxylin and eosin and classified into three groups, the cuboidal (A), elongated (B, arrowheads) and intermediate-type cells (C, arrows). Oligodendrocytoma-like cells are shown in a population of intermediate-type cells (D). Bar=25 μm.

was partially attached to the periventricular brain parenchyma and showed a slight invasion into the brain (Fig. 2B). The epithelial tumor cells had proliferated in solid (Fig. 2B), papillary, cribriform (Fig. 2C) and tubular (Fig. 2D) growth patterns. In the papillary and tubular growing areas, a single layer of papillary epithelial cells covered the fibrovascular connective tissue, as identified by MT staining; the cuboidal tumor cells had round to oval nuclei with no atypia and abundant eosinophilic cytoplasm (Fig. 3A). In the tubular, cribriform or solid growing area, elongated cells mixed with cuboidal cells showed elongated to oval nuclei with mild atypia and eosinophilic cytoplasm (Fig. 3B); furthermore, we observed intermediate-type cells containing pleomorphic nuclei with mild atypia and eosinophilic or pale cytoplasm along with an ill-defined cell border (Fig. 3C). The majority of tumor cells were cuboidal or intermediate cells, followed by elongated cells. In addition to these features, a portion of the intermediate-type cells had a similar appearance as the oligodendroglioma cells. These cells had small round nuclei with scanty eosinophilic to clear fibrillary cytoplasm, similar to a "fried egg", and showed solid growth patterns (Fig. 3D). The average mitotic rate was 0 mitosis in 6 high-power fields (HPFs) in the papillary growing area, 6 mitoses in 10 HPFs in the tubular growing area, 7 mitoses in 10 HPFs in the solid growing area, and 5 mitoses in 10 HPFs in the whole area. MT staining demonstrated that scant interstitial connective tissues had spread between tumor cells throughout the tumor mass. Other organs were not examined histopathologically.

On immunohistochemical examination, many cuboidal tumor cells were strongly positive for epithelial markers including AE1/

Table 1. Primary antibodies and experimental conditions used in our immunohistochemistry experiments

Antigen	Abbreviated name	Host species	Clonality	Clone name	Dilution	Antigen retrieval or/and DNA denaturation	Manufacturer
Beta III Tubulin	-	Mouse	Monoclonal IgG1	TU-20	1:500	Microwaving[b]	Abcam Inc. (Tokyo, Japan)
Cytokeratin AE1/AE3	AE1/AE3	Mouse	Monoclonal IgG1	AE1/AE3	1:50	Autoclaving[a]	Dako (Glostrup, Denmark)
Cytokeratin MNF116	MNF116	Mouse	Monoclonal IgG1	MNF116	1:100	Autoclaving[a]	DakoCytomation (Glostrup, Denmark)
Doublecortin	DCX	Rabbit	Polyclonal IgG	n.a.	1:1,000	None	Abcam Inc. (Tokyo, Japan)
Glial fibrillary acidic protein	GFAP	Mouse	Monoclonal IgG1	GA5	1:200	None	Millipore Corporation (Temecula, CA, U.S.A.)
Ki-67	-	Mouse	Monoclonal IgG1	MIB-1	1:100	Microwaving[c]	Dako (Glostrup, Denmark)
Nestin	-	Mouse	Monoclonal IgG1	Rat 401	1:400	Microwaving[c]	BD Biosciences, Inc. (San Jose, CA, U.S.A.)
Oligodendrocyte transcription factor	OLIG2	Rabbit	Polyclonal IgG	n.a.	1:1,000	None	LifeSpan Biosciences, Inc. (Seattle, WA, U.S.A.)
Podoplanin	-	Rabbit	Polyclonal IgG	D2-40	1:200	Microwaving[b]	Bioss Inc. (Woburn, MA, U.S.A.)
S100	-	Rabbit	Polyclonal IgG	n.a.	1:400	Autoclaving[a]	DakoCytomation (Glostrup, Denmark)
Vimentin	-	Rabbit	Polyclonal IgG	C-20	1:200	Microwaving[b]	Santa Cruz Biotechnology, Inc. (Dallas, TX, U.S.A.)
Von willebrand factor	vWF	Rabbit	Polyclonal IgG	n.a.	1:200	Microwaving[c]	DakoCytomation (Glostrup, Denmark)

n.a., not applicable. a) 121°C for 10 min in Dako target retrieral solution (pH 9.0, Dako). b) 90°C for 10 min in 10 mM citrate buffer (pH 6.0). c) 90°C for 10 min in Dako target retrieral solution (pH 9.0, Dako).
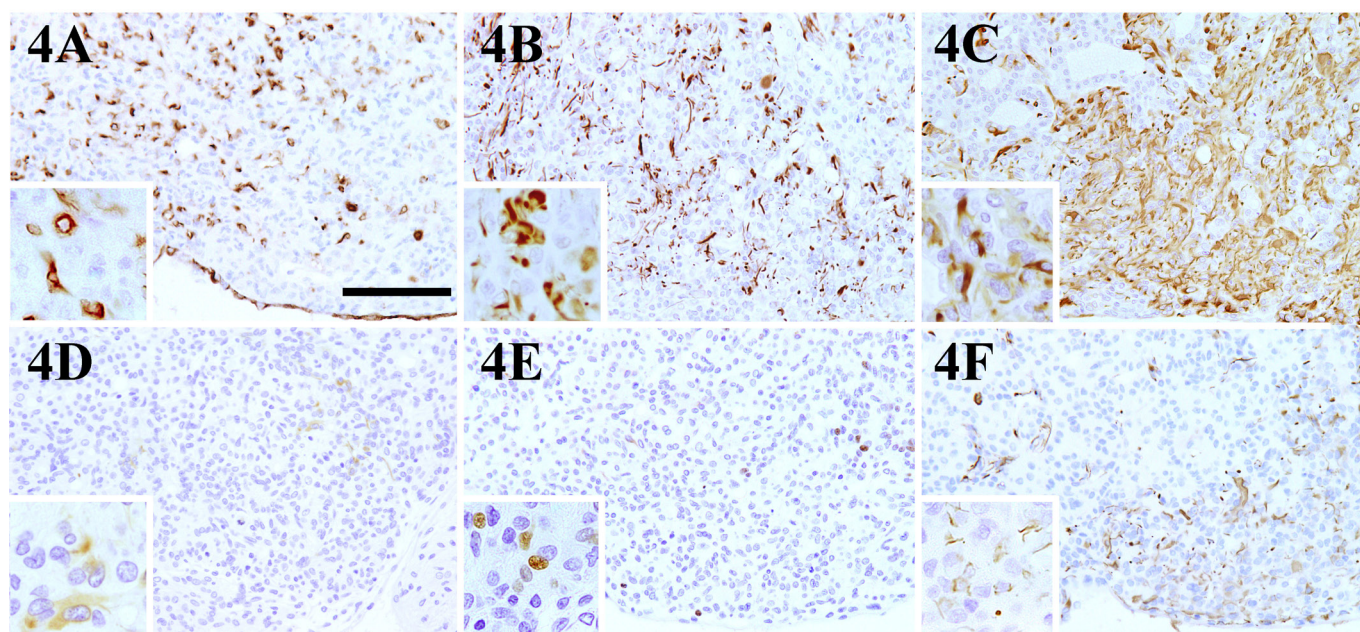
Fig. 4. Immunohistochemical staining of tumor cells for cytokeratin AE1/AE3 (A), vimentin (B), GFAP (C), DCX (D), OLIG2 (E) and nestin (F). Bar=100 μm. The inset shows higher magnification of tumor cells.

AE3 (Fig. 4A) and cytokeratin MNF116 (MNF116). Some cuboidal tumor cells and many elongated and intermediate-type cells tested positive for vimentin (Fig. 4B) and S-100, mesenchymal and nerve fiber markers, respectively. Most elongated cells tested positive for GFAP, an astrocytic marker, and some cuboidal tumor cells and many intermediate-type cells also tested positive for GFAP (Fig. 4C). The cytoplasm of intermediate cells was rarely positive for doublecortin (DCX) (Fig. 4D), a neuronal precursor marker. The nuclei of intermediate cells, especially oligodendroglioma-like cells, were positive for oligodendrocyte transcription factor (OLIG2) (Fig. 4E), an oligodendrocyte and a neural stem cell marker. A small population of cuboidal cells and some elongated and intermediate-type cells tested positive for nestin (Fig. 4F), an astrocytic, a neural stem cell and a glial precursor

Table 2. Immunohistochemical characteristics of the types of tumor cells in the present case compared with tumor cells of choroid plexus carcinomas in dogs and rats and epithelial cells of the choroid plexus in rats

Antigen	Tumor cells in the present case				Tumor cells of CPCs in human[a]	Tumor cells of CPCs in dog[b]	Tumor cells of CPCs in rat[c]	Epithelial cells of the choroid plexus in the present case
	Cuboidal cells	Elongated cells	Intermediate cells	Oligodendroglioma-like cells				
Beta III Tubulin	−	−	−	−	ND	−	ND	−
CK AE1/AE3	++	+	−	−	++	+	ND	++
CK MNF116	−	±	−	−	ND	ND	+	+
DCX	−	±	−	−	ND	−	ND	−
GFAP	+	++	+	−	++	±	−	−
Ki-67	+	+	+	+	++	+	ND	−
Nestin	±	+	+	−	ND	−	ND	−
Olig2	−	+	−	++	ND	ND	ND	−
Podoplanin	−	−	−	−	ND	ND	ND	+
S100	+	+	+	+	++	ND	−	−
Vimentin	±	++	+	−	++	ND	−	−
vWF	−	−	−	−	ND	ND	ND	−

Symbols used are; −, negative; ±, occasionally positive; +, mostly positive; ++, generally positive with strong intensity; CPCs, choroid plexus carcinomas; ND, no data. a) The immunohistochemical result of eight cases of humans studied in the report [1]. b) The immunohistochemical result of three cases of dogs studied in the report [9]. c) The immunohistochemical result of one case of a rat studied in the report [14].

marker. The tumor cells were negative for beta III Tubulin, an early-phase neuronal cell marker and podoplanin, a choroid plexus epithelial cell marker. The cell proliferation activity of tumor cells was 1.8%, as measured by Ki-67 staining. Endothelial cells positive for von Willebrand factor (vWF) were also found in the tumor. A summary of the immunohistochemical examinations is shown in Table 2.

The present tumor mass was accidentally found in the brain section during the process of tissue preparation in a 14-day toxicity study of rat. We observed a slight increase in the brain weight of the rat that might be explained by the presence of growing tumor. The rat had been treated with MNU for 14-days via oral tubules; however, it would be reasonable to suggest that MNU-treatment did not induce brain tumor since this treatment was administered for a short period of 14 days. Therefore, the present case of tumor development was considered spontaneous, as previously seen in a 14-week-old Donryu rat [14].

The gross location of the tumor mass strongly suggested that the tumor might have arisen from choroid plexus or ependymal lining cells. Histopathologically, the cuboidal tumor cells resembled normal epithelial cells of the choroid plexus. There were variations in the cellular architecture, including the papillary, tubular, cribriform or solid growth pattern of epithelial tumor cells. The choroid plexus papilloma was typically characterized by well-developed papillary formation mimicking the normal choroid plexus, while the choroid plexus carcinoma was composed of well-defined papillary structures, complex papillary inholdings, or poorly formed papillae [3, 10]. The tubular, cribriform or solid growth pattern of epithelial tumor cells might be observed as poorly defined papillary structures. Indeed, a solid growth pattern has previously been reported in undifferentiated choroid plexus carcinoma [1]. Furthermore, the tumor cells showed nuclear atypia, increased mitosis and invasion of the surrounding brain parenchyma; cyto-architecture of the malignancy strongly suggested that the present case was a choroid plexus carcinoma. Interestingly, we identified atypical cells, elongated cells or intermediate pleomorphic cells, suggesting as the cyto-architecture features of malignancy. Atypical tumor cells, such as clear cells or rhabdoid cells, have been found in human choroid plexus carcinoma [1]; however, elongated cells and intermediate pleomorphic cells were not reported to our knowledge.

Immunohistochemical analyses also provided evidence that the present case exhibited a complex phenotype of tumor cells. Strong immunoreactivity for AE1/AE3 and vimentin was consistent with the findings in cases in humans and dogs [1, 3, 9]. The positive reactions to vimentin as well as S-100 might be associated with choroid plexus cells being derived from the neuroectodermal plate [6]. In addition, the present case appeared to show glial differentiations. The presence of GFAP-expressing cells suggested that these tumor cells expressed features that might be a prerogative of glial and ependymal cells [1, 9, 17]. GFAP reactivity might be owing to the embryonic nature of tumor cells because the positive reactions were confirmed in the choroid plexus in newborns, infants and children, but not in adults [6]. Furthermore, we identified nestin-expressing cells as an astrocytic, a neural stem cell, or a glial precursor, and OLIG2-expressing cells as neural stem cells or oligodendrocytoma cells in the tumor. Oligodendrocytoma-like cells have previously been reported only by HE stains in human choroid plexus tumors [2].

On the other hand, the tumor also had a characteristic of neuronal differentiations. DCX-expressing neuronal progenitor cells were found in the tumor tissue. To our knowledge, these cells have not been reported in choroid plexus tumors in any species. Neuronal differentiation of choroid plexus tumors has been reported in humans, including children, in which the tumor cells showed immunopositive reactions for neurofilament and neural cell adhesion molecules [5, 7]. The present case may show the initial stage of neuronal differentiation because tumors were partially positive for DCX, a neuronal progenitor cell marker, but negative for beta III Tubulin, an early-phase neuronal cell marker.

We provided an overview of the morphology and immunoreactivities of tumor cells: cuboidal cells had a feature of epithelial cells as expressed AE1/AE3, and elongated cells had a feature of mesenchymal and embryonic cells as expressed vimentin and

GFAP, respectively. The immunoreaction of intermediate cells might mimic that of elongated cells rather than cuboidal cells, since the intermediate cells expressed vimentin and GFAP, but not AE1/AE3. The immunoreactivities of GFAP and nestin were different between tumor cell types, but that of S100 was consistent in each tumor cell. These differentiations may be caused and maintained by changes in the environment, such as the cerebrospinal fluid (CSF), with an occurrence of the choroid plexus tumor, which originally produces the CSF. Choroid plexus epithelial cells are known to gain features, similar to multipotent stem cells, depending on the components of CSF and show glial and/or neuronal differentiation [8].

Comparing our case with the previously reported choroid plexus carcinoma in a 14-week-old Donryu rat [14], tumor cells were similarly immunopositive for MNF116 in both studies; however, the Donryu rat showed a negative reaction to vimentin, S-100 and GFAP. These results suggest that there is heterogeneity among tumor cells even in young adult rats. The present case in a 7-week-old rat might be similar to choroid plexus tumor cases seen in children [6, 7]. The neoplasm had features of neuronal and glial differentiations with cellular complexity, including neural stem cell, neuronal and glial precursors, astrocytic or oligodendrocyte cells, as well as typical choroid plexus epithelial cells. It would be reasonable to assume that a part of the neoplasm was not yet committed to specific differentiation and thus, maintained the characteristics of a stem or progenitor cell; in contrast, most of the choroid plexus tumor cells appeared to undergo or had undergone differentiation to epithelial cells. Thus, it is suggested that tumor cells might be derived from neuroepithelial cells that are multipotent stem cells of the nervous system [12].

REFERENCES

1. Barreto, A. S., Vassallo, J. and Queiroz, L. S. 2004. Papillomas and carcinomas of the choroid plexus: histological and immunohistochemical studies and comparison with normal fetal choroid plexus. *Arq. Neuropsiquiatr.* **62** 3A: 600–607. [Medline] [CrossRef]
2. Burger, P. C. and Rodriguez, F. 2016. Choroid plexus neoplasms. p. 165. *In*: Diagnostic Pathology Neuropathology, 2nd ed. (Kleinschmidt-DeMasters, B. K., Tihan, T. and Rodriguez, F. eds.), Elsevier, St. Louis.
3. Cantile, C., Campani, D., Menicagli, M. and Arispici, M. 2002. Pathological and immunohistochemical studies of choroid plexus carcinoma of the dog. *J. Comp. Pathol.* **126**: 183–193. [Medline] [CrossRef]
4. Chandra, M., Riley, M. G. and Johnson, D. E. 1992. Spontaneous neoplasms in aged Sprague-Dawley rats. *Arch. Toxicol.* **66**: 496–502. [Medline] [CrossRef]
5. Figarella-Branger, D., Lepidi, H., Poncet, C., Gambarelli, D., Bianco, N., Rougon, G. and Pellissier, J. F. 1995. Differential expression of cell adhesion molecules (CAM), neural CAM and epithelial cadherin in ependymomas and choroid plexus tumors. *Acta Neuropathol.* **89**: 248–257. [Medline] [CrossRef]
6. Gaudio, R. M., Tacconi, L. and Rossi, M. L. 1998. Pathology of choroid plexus papillomas: a review. *Clin. Neurol. Neurosurg.* **100**: 165–186. [Medline] [CrossRef]
7. Gianella-Borradori, A., Zeltzer, P. M., Bodey, B., Nelson, M., Britton, H. and Marlin, A. 1992. Choroid plexus tumors in childhood. Response to chemotherapy, and immunophenotypic profile using a panel of monoclonal antibodies. *Cancer* **69**: 809–816. [Medline] [CrossRef]
8. Hashemi, E., Sadeghi, Y., Aliaghaei, A., Seddighi, A., Piryaei, A., Broujeni, M. E., Shaerzadeh, F., Amini, A. and Pouriran, R. 2017. Neural differentiation of choroid plexus epithelial cells: role of human traumatic cerebrospinal fluid. *Neural Regen. Res.* **12**: 84–89. [Medline] [CrossRef]
9. Ide, T., Uchida, K., Kikuta, F., Suzuki, K. and Nakayama, H. 2010. Immunohistochemical characterization of canine neuroepithelial tumors. *Vet. Pathol.* **47**: 741–750. [Medline] [CrossRef]
10. Kaufmann, W., Bolon, B., Bradley, A., Butt, M., Czasch, S., Garman, R. H., George, C., Gröters, S., Krinke, G., Little, P., McKay, J., Narama, I., Rao, D., Shibutani, M. and Sills, R. 2012. Proliferative and nonproliferative lesions of the rat and mouse central and peripheral nervous systems. *Toxicol. Pathol.* **40** Suppl: 87S–157S. [Medline] [CrossRef]
11. Krinke, G. J., Kaufmann, W., Mahrous, A. T. and Schaetti, P. 2000. Morphologic characterization of spontaneous nervous system tumors in mice and rats. *Toxicol. Pathol.* **28**: 178–192. [Medline] [CrossRef]
12. Lun, M. P., Monuki, E. S. and Lehtinen, M. K. 2015. Development and functions of the choroid plexus-cerebrospinal fluid system. *Nat. Rev. Neurosci.* **16**: 445–457. [Medline] [CrossRef]
13. Pace, V. 1998. Spontaneous choroid plexus carcinoma in an albino rat. *Exp. Toxicol. Pathol.* **50**: 225–228. [Medline] [CrossRef]
14. Shimomoto, T., Yoshida, M., Takahashi, M., Uematsu, F., Maekawa, A. and Nakae, D. 2004. A case report of a choroid plexus carcinoma spontaneously occurring in the right lateral ventricle of a 14-week-old, female Donryu rat. *Toxicol. Pathol.* **32**: 264–268. [Medline] [CrossRef]
15. Solleveld, H. A. and Boorman, G. A. 1990. Brain. pp. 155–177. *In*: Pathology of the Fischer Rat. (Boorman, G. A., Eustis, S. L., Elwell, M. R., Montgomery, C. A. and MacKenzie, W. F. eds.), Academic Press Inc., San Diego.
16. Song, R. B., Vite, C. H., Bradley, C. W. and Cross, J. R. 2013. Postmortem evaluation of 435 cases of intracranial neoplasia in dogs and relationship of neoplasm with breed, age, and body weight. *J. Vet. Intern. Med.* **27**: 1143–1152. [Medline] [CrossRef]
17. Taratuto, A. L., Molina, H. and Monges, J. 1983. Choroid plexus tumors in infancy and childhood. Focal ependymal differentiation. An immunoperoxidase study. *Acta Neuropathol.* **59**: 304–308. [Medline] [CrossRef]
18. Thompson, S. W., Huseby, R. A., Fox, M. A., Davis, C. L. and Hunt, R. D. 1961. Spontaneous tumors in the Sprague-Dawley rat. *J. Natl. Cancer Inst.* **27**: 1037–1057. [Medline]